International Journal of the Korean Society of Precision Engineering Vol. 3, No. 4. October 2002.

Polishing Robot Attached to a Machining Center for a Freely-Curved Surface Die

Min-Cheol Lee[1], Seok-Jo Go[2], Young-Gil Cho[3] and Man-Hyung Lee[1]

[1] School of Mechanical Engineering, Pusan National University, Pusan, South Korea
[2] Division of Mechanical Engineering, Dongeui Institute of Technology, Pusan, South Korea
[3] SAMSUNG Electro-Mechanics Co. Ltd., Yonggi-gun, South Chungchong Province, South Korea

ABSTRACT

Polishing a die that has free-form surfaces is a time-consuming and tedious job, and requires a considerable amount of high-precision skill. In order to reduce the polishing time and cope with the shortage of skilled workers, a user-friendly automatic polishing system was developed. The polishing system is composed of two subsystems, a three-axis machining center and a two-axis polishing robot. The system has five degrees of freedom and is able to keep the polishing tool in a position normal to the die surface during operation. A sliding mode control algorithm with velocity compensation was proposed to reduce tracking errors. Trajectory tracking experiments showed that the tracking error can be reduced prominently by the proposed sliding mode control compared to a PD (proportional derivative) control. To evaluate the polishing performance of the polishing system and to find the optimal polishing conditions, the polishing experiments were conducted.

Keywords : Polishing robot, Machining center, Sliding mode control, Optimal polishing conditions

1. Introduction

In the process of die manufacturing, some polishing work must be performed to remove tool marks and to improve the smoothness and flatness of die surfaces. However, the polishing process still depends on the experience of an expert while the cutting process has been automated due to progress in CNC (computer numerical control) and CAD/CAM. Also, even though the expert polishes a die, it takes a lot of time to obtain the required degree of roughness and smoothness. Therefore, it represents a major problem because the polishing process consumes 30~40 % of the total die-manufacturing time [1-3]. Moreover, workers tend to avoid the polishing workplace because of the excessive exposure to dust and noise [1-4]. Therefore, to improve productivity and to solve the potential shortage of skilled workers, several studies on the automation of the polishing process have been conducted [1-8]. Many companies also need an automated process because of the shortage of workers and high labor costs. Some researchers developed a five-axis articulated polishing robot to reduce the cost. The robot, however, has some defects in its stiffness and position accuracy [6,7].

In this study a polishing system was developed to automate the polishing process and to cope with the shortage of skilled workers. The developed polishing system consists of a linear motion part with three degrees of freedom and a rotative motion part with two degrees of freedom. The latter part is a polishing robot and is attached to the linear motion part of a prevailed machining center in industry. Thus, this system has five degrees of freedom. To improve the polishing performance, the polishing system can maintain the polishing tool normal to the die surface and a constant pressure during operation. This polishing system has several advantages: reduced time for setting polishing work, decreased labor costs, effective operation, continuous polishing work without an operator,

improved machine accuracy, and the ability to polish a free curved surface die.

The contact force of a polishing robot, which is caused by removing tool marks and rotating the polishing tool, always changes [8-10]. Unless these disturbances to the polishing robot are properly compensated for, the trajectory control performance cannot be satisfied. The PID (proportional integral derivative) control algorithm is the most common type of industrial robot controllers. However, the algorithm does not provide the compensation capability needed, especially when sudden changes in the set parameters frequently occur. Unless the nonlinearities of robot manipulators are completely compensated for, a satisfactory control performance cannot be expected from the PID algorithm. Moreover, developing an accurate model for the robot system is difficult because of the nonlinear friction effect and changes in the payload during task executions [11,12].

In the previous study, in order to reduce the tracking errors related to the unmodeled dynamics in the operation of the polishing robot, the sliding mode control algorithm was implemented on a polishing robot [13]. However, the algorithm could not reduce the inherent chattering which was caused by excessive switching input around the sliding surface. Therefore, this study designs the sliding mode control algorithm with velocity compensation to reduce chattering in the sliding mode control and to provide a robust trajectory tracking performance in the operation of the polishing system.

A desired polishing data is generated by PolyCAM, a dedicated CAM software for the polishing system. Since the polishing system is composed of two subsystems such as polishing robot and machining center, the host computer must transmit the generated polishing data to the FANUC controller of the machining center and the DSP controller of the polishing robot. Thus, the three-axis trajectory data for the machining center and the two-axis trajectory data for the polishing robot are separated from the generated five-axis polishing data by the code separation program. The code separation program was developed in the Windows environment to separate the NC code easily. And, in order to evaluate the polishing performance of the polishing system and to find the optimal polishing conditions, the polishing experiments on a shadow mask die were conducted.

2. Automatic Polishing System

2.1 Two-axis Polishing Robot

To polish a die with free-form surfaces basically requires a mechanism with more than five degrees of freedom [6]. It is difficult for a mechanism with three degrees of freedom to polish such a die uniformly. The polishing tool cuts the polishing surface more deeply as the contact surface grows smaller. In order to solve this problem, a universal joint or a ball joint was used. However, the polishing performance is poor because the distribution of a contact force changes while the slope of the free surface changes. Therefore, we need more than three degrees of freedom to maintain the polishing tool normal to the free surface die. A mechanism with five degree of freedom maintains the polishing tool normal to the free surface. In this case, the polishing performance is improved because the contact force is distributed uniformly although the slope of the free surface has changed. A mechanism with five degrees of freedom allows it to polish the various free surfaces. Therefore, the articulated polishing robot with five axes was selected and developed [6-8].

The robot, however, had some defects regarding its stiffness and position accuracy. To minimize these defects, the two-axis polishing robot attached to a three-axis machining center was developed. The structure and appearance of the polishing robot is shown in Fig. 1. The polishing robot is composed of actuators to drive the robot, a pneumatic motor to rotate the polishing tool, a pneumatic cylinder to maintain the polishing tool normal to the die surface, and a tool adapter for attaching the polishing robot to a machining center. The specifications for the polishing robot are listed in Table 1. The tool adapters are shown in Fig. 2.

2.2 Five-axis Polishing System

The polishing system was developed to automate the polishing process. The system is composed of a three-axis machining center and a two-axis polishing robot attached to the machining center as shown in Fig. 3. The machining center is controlled by the FANUC

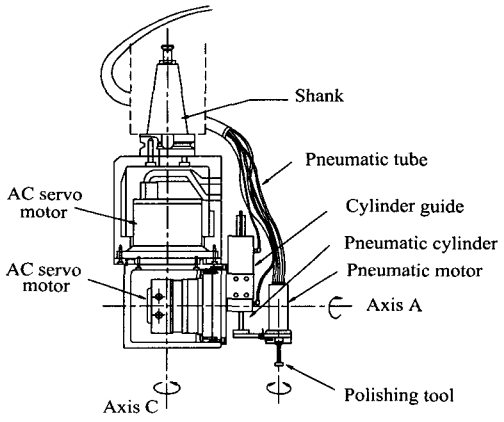

Fig. 1(a) Structure of a polishing robot

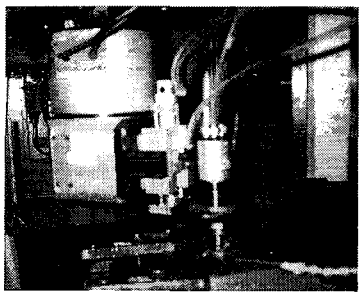

Fig. 1(b) Appearance of a polishing robot

controller, and the polishing robot by a DSP controller.

A host computer uses the CAM software to generate polishing trajectory data on the polishing system. Since the polishing system is composed of two subsystems, the host computer must transmit the generated polishing data to the FANUC controller and the DSP controller through a serial port and a DPRAM (dual port RAM), respectively.

The polishing tool is controlled by the DSP controller to maintain it normal to the die surface. The pneumatic cylinder presses the polishing tool into the die surface with constant force. At the same time, the polishing tool is rotated by the pneumatic motor and does the polishing work. These processes are synchronized with the machining center. In order to synchronize the start points of each polishing trajectory for the machining center and the polishing robot, the M51 and the SM2 terminal of the machining center are connected to the DIO (digital input output) ports of the DSP controller. A flow chart for the operation of the polishing system is shown in Fig. 4.

Table 1 Specifications of polishing robot

Item	Specification	Maker	Model type
Actuator	Harmonic drive	Harmonic drive systems	FHA-17A
Rotation of tool	Pneumatic motor	FUJI	F-6SM-28R
Polishing force	Single cylinder	FESTO	DSN-25-50-PPV
Control unit	DSP controller	TI	TMS320C40

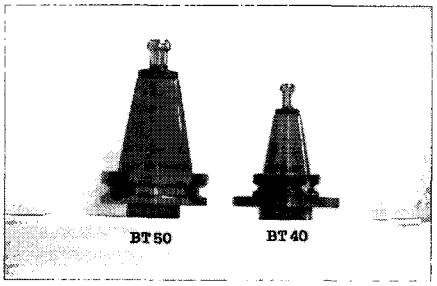

Fig. 2 Tool adapters for attaching the polishing robot to a machining center

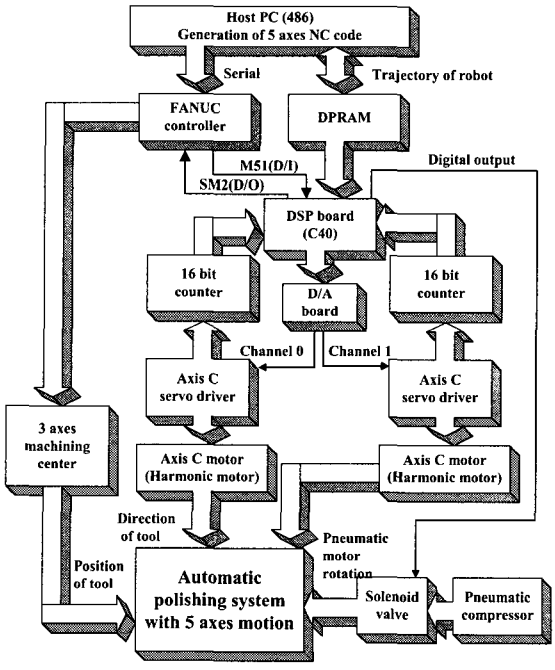

Fig. 3 Schematic diagram of the polishing robot system

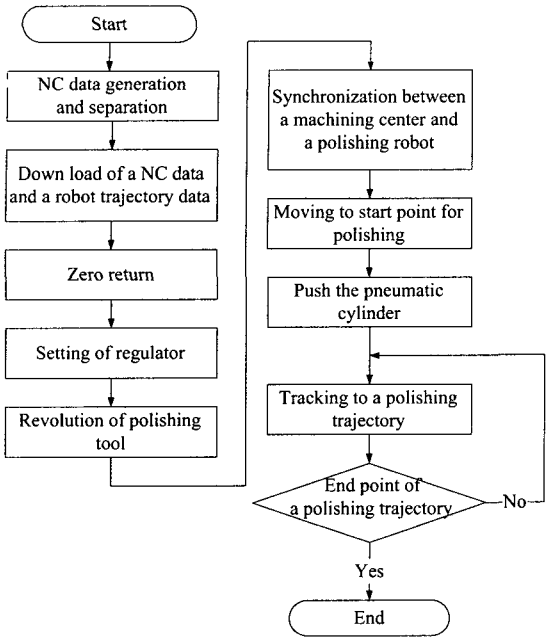

Fig. 4 Flow chart for operation of the polishing system

The developed polishing system is able to reduce the number of steps in the polishing process and improve the surface roughness and waviness.

3. Design of Sliding Mode Control

The contact force of a polishing robot, which is caused by removing tool marks and rotating the polishing tool, always changes [8-10]. Unless these disturbances to the polishing robot are properly compensated for, the trajectory control performance cannot be satisfied. Thus, this study designs the sliding mode control algorithm with velocity compensation to reduce chattering in the sliding mode control and to provide a robust trajectory tracking performance in the operation of the polishing system.

3.1 Sliding Mode Control with Velocity Compensation

The simplified dynamic equation of the polishing robot is written as follows [9,10,13].

$$J_i \ddot{\theta}_i + B_i \dot{\theta}_i + F_i = k_i u_i \qquad (1)$$

where J_i is the summation of all linear terms in the moment of inertia of the link i and the driving motor, and B_i is the equivalent damping coefficient from the motor, reduction gears, and the viscous friction of the link i. The disturbance term F_i is the summation of the nonlinear terms of the inertia moments, the Coriolis and centrifugal force, the gravity force, and the Coulomb friction term. The k_i is the constant determined from the motor torque coefficient, reduction rate of gears, and armature resistance. Finally, u_i is the control input voltage.

The control input of the sliding mode controller could easily be obtained from the simplified dynamic Eq. (1). Let the desired angle and angular velocity of the link, i, be denoted by θ_{di} and $\dot{\theta}_{di}$, respectively, and the corresponding measured angular quantities denoted by θ_i and $\dot{\theta}_i$, respectively. The error equations are written as

$$e_i = \theta_i - \theta_{di}, \quad \dot{e}_i = \dot{\theta}_i - \dot{\theta}_{di} \qquad (2)$$

A switching line for the sliding mode is expressed as

$$s_i = c_i e_i + \dot{e}_i \qquad (3)$$

where s_i is the switching line of the link i and c_i is the corresponding slope.

In order to satisfy the existence condition of the sliding mode, when the unmodeled nonlinear terms are replaced by disturbances, a control input is proposed as follows:

$$u_i = \psi_{ai} e_i + \psi_{\beta i} \dot{e}_i + \psi_{fi} \qquad (4)$$

$$\psi_{ai} = \begin{cases} \alpha_{1i} & \text{if } s_i e_i > 0 \\ \alpha_{2i} & \text{if } s_i e_i < 0 \end{cases}$$

$$\psi_{\beta i} = \begin{cases} \beta_{1i} & \text{if } s_i \dot{e}_i > 0 \\ \beta_{2i} & \text{if } s_i \dot{e}_i < 0 \end{cases}$$

$$\psi_{fi} = \begin{cases} u_{fi}^{-} = M_{1i} + M_{2i} |e_i| & \text{if } s_i > 0 \\ u_{fi}^{+} = -M_{1i} - M_{2i} |e_i| & \text{if } s_i < 0 \end{cases}$$

where $\psi_{\beta i}$ is the control input term, which ensure the existence condition of the sliding mode, to compensate for unfavorable effects due to the velocity error $\dot{e}_i$ on

the trajectory tracking. The control input term to compensate for disturbances is ψ_{fi}.

A sliding mode at the link i exists when the condition $s_i \dot{s}_i < 0$ is satisfied. From Eqs. (1) and (4), the condition is derived as follows:

$$
\begin{aligned}
s_i\dot{s}_i &= s_i(c_i\dot{e}_i + \ddot{e}_i) \qquad (5)\\
&= s_i\left\{c_i\dot{e}_i + \frac{k_i}{J_i}u_i - \frac{B_i}{J_i}(\dot{e}_i + \theta_{di}) - \frac{F_i}{J_i} - \dot{\theta}_{di}\right\}\\
&= s_i\left\{c_i\dot{e}_i + \frac{k_i}{J_i}\psi_{ai}e_i + \frac{k_i}{J_i}\psi_{\beta i}\dot{e}_i + \frac{k_i}{J_i}\psi_{fi} - \frac{B_i}{J_i}\dot{e}_i - \frac{\overline{F_i}}{J_i}\right\}\\
&= s_ie_i\left(\frac{k_i}{J_i}\psi_{ai}\right) + s_i\dot{e}_i\left(c_i + \frac{k_i}{J_i}\psi_{\beta i} - \frac{B_i}{J_i}\right)\\
&\quad + s_i\left(\frac{k_i}{J_i}\psi_{fi} - \frac{\overline{F_i}}{J_i}\right) < 0
\end{aligned}
$$

where, $\overline{F_i} = F_i + \frac{B_i}{J_i}\theta_{di} + \dot{\theta}_{di}$

If all of the terms in Eq. (5) are negative, the condition is always satisfied. Equation (5) is also used to obtain the limit values of all of the switching parameters in Eq. (4). When the first term in Eq. (5) is negative, the limit values of the switching parameters ψ_{ai}, $\psi_{\beta i}$, and ψ_{fi} are derived as follows:

$$
\begin{cases}
\frac{k_i}{J_i}\psi_{ai} > 0 & \text{if } s_ie_i < 0\\
\frac{k_i}{J_i}\psi_{ai} < 0 & \text{if } s_ie_i > 0
\end{cases} \qquad (6a)
$$

$$
\begin{cases}
c_i + \frac{k_i}{J_i}\psi_{\beta i} - \frac{B_i}{J_i} < 0 & \text{if } s_i\dot{e}_i > 0\\
c_i + \frac{k_i}{J_i}\psi_{\beta i} - \frac{B_i}{J_i} > 0 & \text{if } s_i\dot{e}_i < 0
\end{cases} \qquad (6b)
$$

$$
\begin{cases}
\frac{k_i}{J_i}\psi_{fi} - \frac{\overline{F_i}}{J_i} < 0 & \text{if } s_i > 0\\
\frac{k_i}{J_i}\psi_{fi} - \frac{\overline{F_i}}{J_i} > 0 & \text{if } s_i < 0
\end{cases} \qquad (6c)
$$

To determine the switching parameters ψ_{ai}, $\psi_{\beta i}$, and ψ_{fi} in Eq. (6), the values of inertia J_i and damping coefficient B_i of the robot system are estimated by the signal compression method which identifies unknown parameters of a system [14]. By using the signal compression method, the unknown parameters of the polishing robot are estimated as listed in Table 2. When

Table 2 System parameters of robot

	ω_{ni} (rad/sec)	ξ_i	J_i (Kg m^2)	B_i (Kg m^2/s)
Axis A	12	0.4	0.0114	0.10944
Axis C	12	0.1	0.0991	0.23784

Table 3 Switching parameters for sliding mode

	ψ_α	ψ_β	M_1	M_2
Axis A	-11.04	-0.4	1	0.5
Axis C	0	-4.6	4	1

slopes of the switching line are $c_1 = 5$ and $c_2 = 8$, the limit values of the switching parameters that satisfy the existence condition of sliding mode are derived as listed in Table 3.

For the multi-input sliding mode control, the switching control input should be supplied by a control hierarchy method [15]. The control hierarchy used in this study is a hybrid method that can eliminate the effects of gravity at each link and the interactions between the links. The hybrid method switches proportional control to sliding mode control for links of the lower order as soon as the links of the higher order come into quasi-sliding mode. That is, if the state variables of the higher order satisfy $|s_i| < \varepsilon_i$, those of the lower order enter the sliding mode, thus all of the state variables of the lower order gradually enter the sliding mode. After the sliding mode occurs at axis C, the sliding mode occurs at axis A.

The phase plane for the error states of each link is shown in Fig. 5. Line o-o is the switching line of $s_i = 0$. Lines c-c and d-d are the additional lines used to determine whether the higher order class converges to the sliding mode in the hierarchical control or not. The magnitude of chattering, which is the distance between the switching line and the state variable, is denoted by D and expressed as

$$D = \frac{|c_ie_i + \dot{e}_i|}{\sqrt{c_i^2 + 1}} \qquad (7)$$

A pre-determined dead zone is introduced and its width is described by $D = \varepsilon$ between lines a-a and b-b to reduce the chattering. Reduction of chattering can be

made by changing the value of M_{1i} in ψ_{fi} of control input to a smaller value once the state variable falls into the dead zone [15-17].

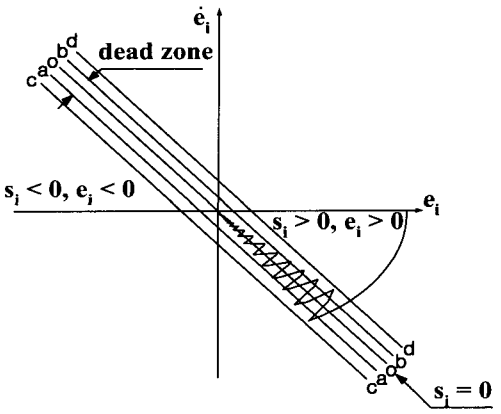

Fig. 5 Phase plane with a pre-determined dead zone around the switching line

3.2 Trajectory Tracking Control

To investigate the trajectory tracking performance of the proposed sliding mode control algorithm, the algorithm is compared with a PD control algorithm, which has been widely used in robot controllers. The desired polishing trajectory of a part of the die of a shadow mask is generated by CAM software.

First, a trajectory tracking control experiment was performed by a PD control. Control gains of the PD control were determined by an expert in robot systems. The experimental results of each axis are shown in Figs. 6 and 7. In the polishing process, the maximum error of axes A and C are 0.45 degrees and 2.5 degrees, respectively.

Second, the trajectory tracking control experiment was performed by the proposed sliding mode control. The experimental results of the sliding mode control are shown in Figs. 8 and 9. By comparing Figs. 6 and 7 with Figs. 8 and 9, it can be shown that the proposed sliding mode control reduces the tracking error more effectively than the PD control does. In Fig. 9, the maximum error of axis C is 0.2 degrees. However, it is possible to correct this error because the structure of the polishing tool has some flexibility and the tool is always in contact with a polishing surface by a constant polishing force.

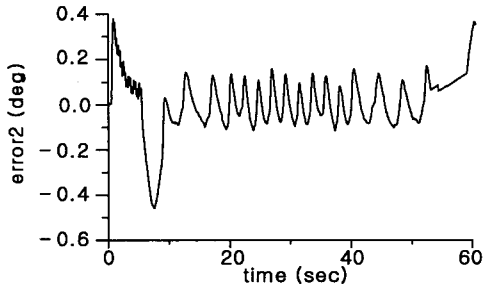

Fig. 6 Trajectory tracking error of axis A by the PD control

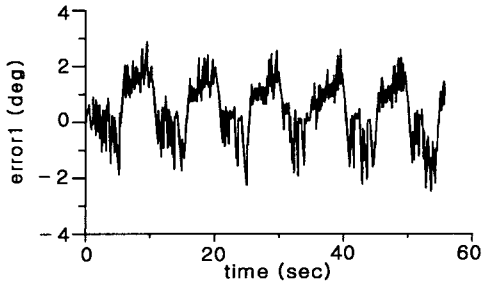

Fig. 7 Trajectory tracking error of axis C by the PD control

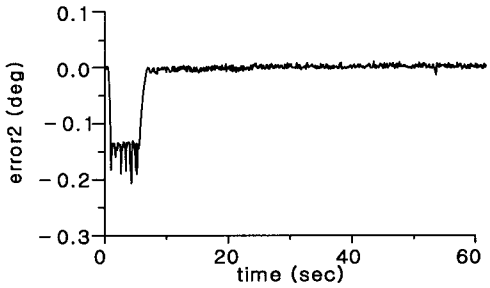

Fig. 8 Trajectory tracking error of axis A by the sliding mode

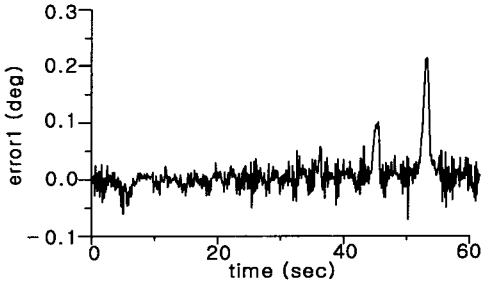

Fig. 9 Trajectory tracking error of axis C by the sliding mode

4. Separation of a Five-axis NC Data

A desired polishing data is generated by PolyCAM, a dedicated CAM software for the polishing system. The polishing conditions are listed in Table 4. Fig. 10 shows a five-axis trajectory of the shadow mask die generated from PolyCAM.

Since the polishing system is composed of two subsystems such as polishing robot and machining center, the host computer must transmit the generated polishing data to the FANUC controller of the machining center and the DSP controller of the polishing robot. Thus, the three-axis trajectory data for the machining center and the two-axis trajectory data for the polishing robot are separated from the generated five-axis polishing data by the code separation as shown in Fig. 11. The polishing trajectory data on a five-axis polishing system is on the left side of the screen. The NC data on a three-axis machining center is on the middle side. The trajectory data on a two-axis polishing robot is displayed on the right side. The code separation program was developed in the Windows environment to separate the NC code easily.

A five-axis NC data is composed of a position data (X, Y, Z) on a machining center, a orientation data (A, C) on a polishing robot, and a feed-rate of a polishing tool. To make a trajectory data on a polishing robot, the developed code separation program only selects a orientation data (A, C), and a reference time is calculated by a feed-rate data for synchronizing. The NC data on a machining center is modified to make a NC code form of FANUC controller.

5. Optimal Polishing Conditions and Evaluation of Polishing Performance

In order to evaluate the polishing performance of the polishing system and to find the optimal polishing conditions, the polishing experiments on a shadow mask die were conducted.

Since polishing work is performed to remove tool marks and to improve the smoothness and flatness of die surfaces, it is important to select a polishing tool. In this study, the polishing tool composed of a ball joint of Nagasei company of Japan and the polishing sheet were developed. The polishing sheets are an embossed

Table 4 Items of polishing conditions

Item	Input
Cutter shape	Dia, Fillet-radius, Length
Path interval	Value
Cutting tolerance	Value
Surface offset	Value
Start point	X, Y, Z position
Clearance height	Inc/Abs, Value
Approach height	Value
Approach and exit type	Xyplane / Tangent
Path type	Single, Zigzag
Path connection	Direct, Jump
Feed rate	Approach, First, Last, Connection value
Spindle speed	Value

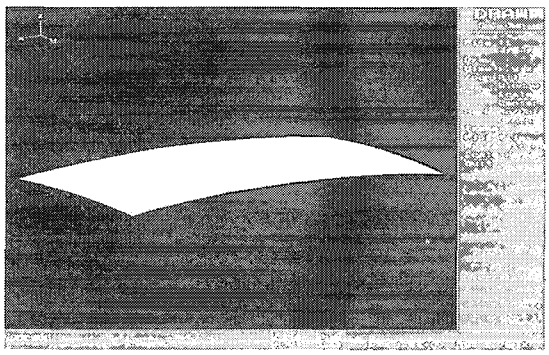

Fig. 10 Trajectory for a shadow mask die

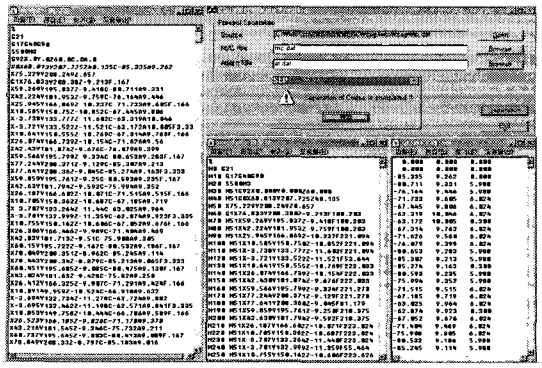

Fig. 11 Separated results

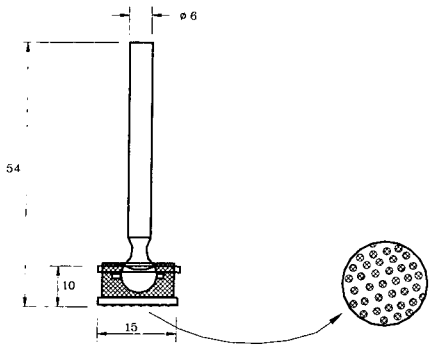

Fig. 12 Polishing tool of a ball-joint type

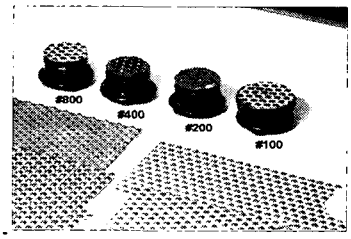

Fig. 13 Polishing sheets

type which puts an abrasive grain in the flexible fiber. Structure of a polishing tool is shown in Fig. 12 and the polishing sheets are shown in Fig. 13.

In order to find optimal polishing conditions, the various polishing experiments of the die of shadow mask (250 mm × 145 mm) were carried out. To find the character of polishing according to a direction of a polishing trajectory, polishing experiments of the same polishing direction and the cross polishing direction are carried out. And, effects of the polishing sheet, the polishing force, the velocity of revolution of a polishing tool, the feed-rate, and numbers of polishing are considered as shown in Figs. 14 and 15. The magnitude of each cell is 30 [mm] ×20 [mm]. The material of the shadow-mask die is STD. The roughness of the cell surface is measured as the number of polishing is increased.

First, to investigate the change of the roughness of the polished surface according to a direction of a polishing trajectory, polishing experiments of the ruled surface and the shadow mask are carried out. After two dies are polished by a number 200 polishing sheet, polishing work is performed according to the polishing conditions as listed in Table 5. The measured results

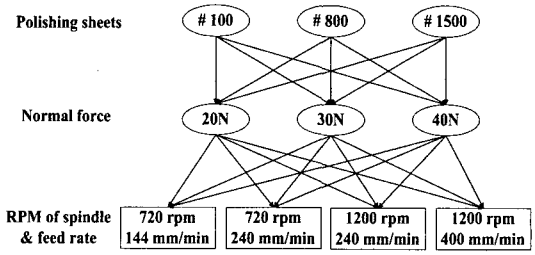

Fig. 14 Polishing conditions

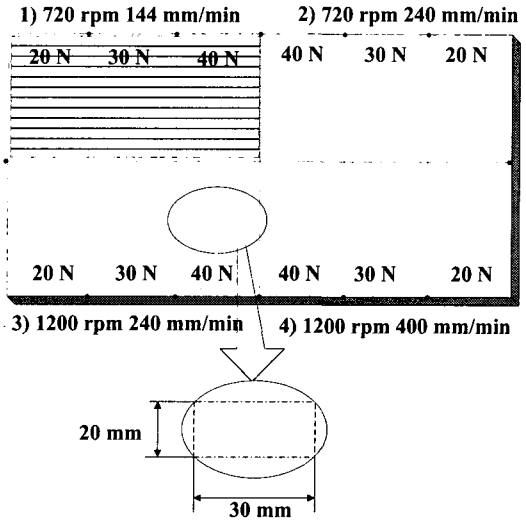

Fig. 15 Polishing area

Table 5 Polishing conditions

Direction	Single	Cross
Force	15N	
Tool(mesh)	R = 5mm (#800)	
Spindle	800 rpm	
Feed-rate	100 mm/min	
Pick-feed	0.5 mm	

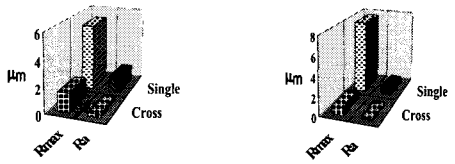

(a) Ruled surface (b) Shadow mask

Fig. 16 Roughness according to polishing direction

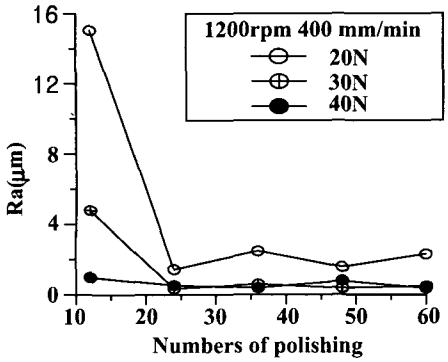

Fig. 17 R_a by the polishing force and the number of polishing at 100 [mesh]

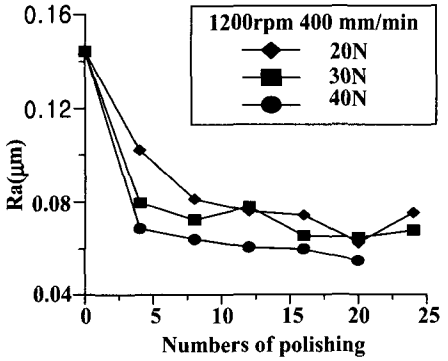

Fig. 18 R_a by the polishing force and the number of polishing at 800 [mesh]

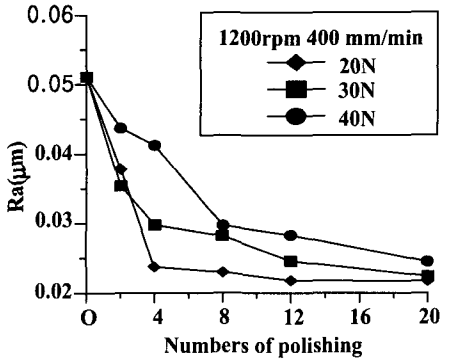

Fig. 19 R_a by the polishing force and the number of polishing at 1500 [mesh]

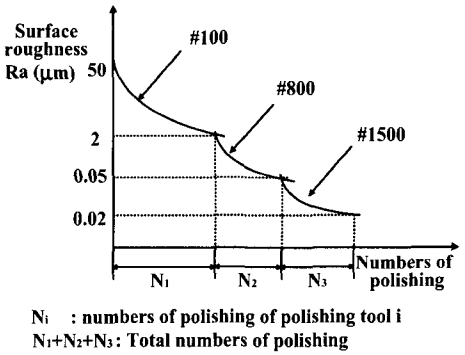

Fig. 20 R_a according to the number of polishing and the polishing sheet

are shown in Fig. 16. In Fig. 16, the polishing experiment of the same polishing direction is named a single and the polishing experiment of the cross polishing direction is named a cross. In case of the shadow mask, R_a of the single is 0.55 [μm] and R_a of the cross is 0.08 [μm]. That is, it is known that the surface roughness by the cross polishing direction is better than the same polishing direction since the regular tool mark is formed by the same polishing direction.

Second, to find the character between the surface roughness and the number of polishing, the surface roughness is measured as the number of polishing is increased. The velocity of revolution of a polishing tool is 1200 [rpm] and the feed-rate is 400 [mm/min]. Figure 17 shows the experimental results at a number 100 polishing sheet. Figures 18 and 19 show the experimental results at 800 [mesh] and 1500 [mesh], respectively. In Fig. 17, the roughness of the cell surface is exponentially better as the number of polishing is increased. However, the surface roughness is rarely changed after the number of polishing reaches about 25. This value is called the critical number of polishing and the surface roughness reaches about 0.5 [μm]. Therefore, the polishing sheet must be changed to improve the surface roughness. In Figs. 18 and 19, at the same method, the critical numbers of polishing is about 4 and the surface roughness reaches about 0.07 [μm] and 0.025 [μm], respectively. As a result, Fig. 20 shows the change of the surface roughness as the number of the polishing sheet and the number of polishing are increased. In Fig. 20, to reduce the number of polishing, it must be used a number 400 polishing sheet after a number 100 polishing sheet since the surface roughness is rarely changed after the number of polishing reaches the critical value.

Third, to find the character between the surface roughness and the polishing force, the efficiency of

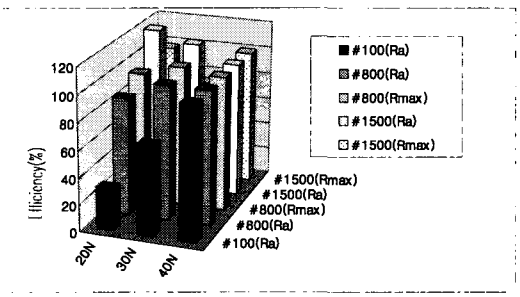

Fig. 21 Efficiency of polishing according to the polishing force

polishing is defined as follows:

$$efficiency_F(\%) = \frac{1}{\frac{roughness_F}{roughness_{40N}}} \times 100 \quad (8)$$

In Eq. (8), $roughness_{40N}$ is the surface roughness at the 40 [N]-polishing force and the efficiency of polishing at the 40 [N] is 100 %. Figure 21 shows the efficiency of polishing according to the polishing force. In Fig. 21, in case of using 100 [mesh], the efficiency of polishing is best at 40 [N]. Oppositely, in case of using 1500 [mesh], the efficiency of polishing is best at 20 [N]. Therefore, to improve the efficiency of polishing, the polishing force must be reduced as the number of the polishing sheet increases.

Finally, to find the character between the surface roughness and the velocity of the polishing tool, it is counted the number of polishing to be reached at the reference value of a R_a and a R_{max}. The polishing experiment is carried out according to the polishing conditions as listed in Table 6. In case of 800 [mesh], the number of polishing is 20 times at 720 [rpm] and 12 times at 1200 [rpm]. And, the same result is obtained at 1500 [mesh]. Therefore, to reduce the number of polishing, it must be increased the velocity of the polishing tool. However, when the velocity of the polishing tool is over 1200 [rpm], the polished surface is singed black. The reason is that the heat is generated by friction between the polishing tool and the surface of a die. Thus, the velocity of the polishing tool is restricted to 1200 [rpm] to prevent the tool from singeing the surface of the die.

These experiment results show that the efficiency of polishing is improved by properly selecting polishing conditions: the polishing force, numbers of polishing, the polishing sheet, and the velocity of the polishing tool. The surface of the polished die is shown in Fig. 22. The results of a polishing experiment show that the polished surface is as smooth as a mirror and that the developed polishing system provides a reliable polishing performance.

Table 6 Efficiency of polishing according to the velocity of the polishing tool

Polishing sheet [mesh]	Items	Reference value [㎛]	Polishing force [N]	Numbers of polishing	
				720 [rpm]	1200 [rpm]
800	R_a	0.05	30	20	12
	R_{max}	0.3		20	12
1500	R_a	0.025	20	8	4
	R_{max}	0.24		20	8

Fig. 22 Shadow mask die after final polishing

6. Conclusion

To reduce the polishing time and to cope with the shortage of skilled workers, a polishing system was developed in this study. And, to solve the problem of tracking errors related to the unmodeled dynamics in the operation of the polishing robot, this study proposed a sliding mode control algorithm that compensates for velocity. To investigate the trajectory tracking performance of the proposed sliding mode control algorithm, the algorithm was compared with the PD control algorithm, which has been used as the most

common type of industrial robot controllers. Results obtained from the trajectory tracking experiments have shown that the proposed sliding mode control reduced the tracking error more effectively than the PD control did, thus providing reliable tracking performance during the polishing process. Also, to find the optimal polishing conditions, the polishing experiments on a shadow mask die were carried out. The experimental results show that the efficiency of polishing is improved by properly selecting polishing conditions: the polishing force, the number of polishing, the polishing sheet, and the velocity of the polishing tool. The results of a polishing experiment show that the polished surface is as smooth as a mirror and that the developed polishing system provides a reliable polishing performance.

Acknowledgment

This research was financially supported by the Korea Science and Engineering Foundation (KOSEF) through the Engineering Research Center for Net Shape and Die Manufacturing at Pusan National University and by the Brain Korea 21 Project.

References

1. M. Kazutoyo, K. Tsukasa, I. Satoru, S. Katsumasa, and S. Tetuo, "Study on Automatic Polishing of Injection Mold- Polishing with constant pressure under controlled tool staying time-," Proc. of the ABTEC, pp. 431-434, 1995.
2. G. M. Park, J. H. Jang, and C. S. Han, "A study on the Experimental Analysis of the Automatic Fine Polishing System," J. of KSPE, Vol. 12, No. 9, pp. 30-39, 1995.
3. M. Suziki, S. Ichiyasu, K. Kirii, S. Sunahara, T. Sakuta, and A. Asai, "Development of Die-finishing Robotic System Controlled by CAD/CAM System," JSPE-58-08, pp. 1309-1314, 1992.
4. S. C. Kang, M. S. Kim, and K. I. Lee, "Development and Verification of a Robot Off-line Programming System for Die Polishing Process," J. of KSPE, Vol. 14, No. 1, pp 69-77, 1997.
5. M. Kunieda, T. Nakagawa, and T. Higuchi, "Robot Polishing of Curved Surface with Magnetically Pressed Polishing Tool," JSPE, Vol. 54, No.1, pp. 121-125, 1988.
6. Y. S. Oh and B. S. Ryuh, "The Development of Grinding Robot System Using NC Data and Off-Line Programming," J. of KSPE, Vol. 16, No. 3, pp. 9-17, 1999.
7. S. J. Park, S. H. Lee, K. S. Ryu, B. S. Sin, D. S. Choi, and D. H. Kim, Development of an Integrated Design and Machining System for 3-D Surface, Final Report, KIMM, 1993.
8. K. Shunichi, A. Tojiro, and L. Ichiro, "Development of a Robot-Polishing System (Polishing Force Control by Means of Fuzzy Set Theory)," JSME J. Series C, Vol. 57, No 543, pp. 3714-3719, 1991.
9. M. C. Lee, Y. G. Cho, and M. H. Lee, "Evaluation of Polishing Performance Using the Improved Polishing Robot System Attached to Machining Center," J. of KSPE, Vol. 16, No. 9, pp. 179-190, 1999.
10. M. C. Lee, S. J. Go, M. H. Lee, C. S. Jun, D. S. Kim, K. D. Cha, and J. H. Ahn, "A Robust Trajectory Tracking Control of a Polishing Robot System Based on CAM Data," Int. J. of RCIM, Vol. 17:1-2, pp. 177-183, 2001.
11. K. S. Fu, R. C. Gonzalez, and C. S. G. Lee, Robotics, McGraw-Hill, 1987.
12. K. Nishimoto, "DSP and Its Application to Robot Control," J. of the Robotics Society of Japan, Vol. 7, No. 3, pp. 339-345, 1985.
13. M. C. Lee, and D. J. Ha, "A Study on the Development of Polishing Robot System Attached to Machining Center for Curved Surface Die," J. of KSPE, Vol. 16, No. 4, 1999.
14. M. C. Lee, and N. Aoshima, "Identification and Its Evaluation of the System with a Nonlinear Element by Signal Compression Method," Trans. of SICE, pp. 729-736, 1989.
15. M. C. Lee and N. Aoshima, "Real Time Multi-Input Sliding Mode Control of a Robot Manipulator Based on DSP," Proc. of SICE, pp. 1223-1228, 1993.
16. M. C. Lee, and S. J. Go, " Real Time Fuzzy-Sliding Mode Control for SCARA Robot Based on DSP," Proc. of 2nd Asian Control Conference, pp. 599-602, 1997.
17. M. C. Lee, K. Son, J. M. Lee, "Improving Tracking Performance of Industrial SCARA Robots Using a New Sliding Mode Control Algorithm," KSME I. J., Vol. 12, No. 5, pp. 761-772, 1998.